Self-assembly of amphiphiles into vesicles: A Brownian dynamics simulation

Hiroshi Noguchi* and Masako Takasu
Department of Applied Molecular Science, Institute for Molecular Science, Okazaki 444-8585, Japan
(Received 14 May 2001; published 24 September 2001)

We studied the vesicles of amphiphilic molecules using a Brownian dynamics simulation. An amphiphilic molecule is modeled as the rigid rod, and the hydrophobic interaction is mimicked by the local density potential of the hydrophobic particles. The amphiphilic molecules self-assemble into vesicles with bilayer structure. The vesicles are in fluid phase, and we calculated the lateral diffusion constant and the rate of the flip-flop motion of molecules in vesicles. The self-assembly kinetics into vesicles was also investigated.

DOI: 10.1103/PhysRevE.64.041913 PACS number(s): 87.16.Dg, 87.16.Ac, 82.70.Uv

I. INTRODUCTION

Amphiphilic molecules such as lipids and detergents consist of two parts; a hydrophilic ''head'' and a hydrophobic ''tail.'' The aggregates of amphiphilic molecules in aqueous solution have various structures such as micelles, bilayer membranes, and bicontinuous cubic structure [1,2]. In those structures, the closed bilayer membranes, vesicles, are important biologically as the simple model systems of plasma membrane and other components in cell. The fusion and the fission events of these vesicles occur in the various biological processes, such as exocytosis, endocytosis, protein trafficking, fertilization, and viral infection [3–6].

The various morphologies of vesicles are understood by the coarse-grained surface models where the bilayer membrane is treated as smooth continuous surface [1,2,7–9]. However, in these models, the membranes are assumed as the thin surface, and the molecular structures are not taken into account explicitly. In these models, the artificial recombination of surfaces is needed to investigate the shape transformation with topological change.

The self-assembly of amphiphilic molecules has been studied by the molecular simulations with off-lattice [10–16] and lattice models [17,18]. The molecular simulations with atomic resolution [10–13] have been applied only for the small number of molecules and short-time dynamics due to the restriction of computational time. Thus, some studies used the coarse-grained amphiphilic molecules to investigate self-assembly into vesicles [15,16,18]. However, the models in Refs. [15] and [16] are not applicable to nonbilayer structure such as the fusion intermediates, since a pair of faced amphiphilic molecules is approximated as one object. In Ref. [18], the dynamical property was unclear since they used the square lattice model. Thus, the self-assembly processes remain not sufficiently understood.

The purpose of the present study is the establishment of the simple molecular model for vesicles with bilayer structure and the investigation of the properties of self-assembly. We used three-dimensional Brownian dynamics of rigid amphiphilic molecules. The hydrophobic interaction is mimicked by the multibody local density potential of the hydrophobic particles.

*Email address: noguchi@ims.ac.jp

This paper is organized as follows. In Sec. II, we describe our simulation model and methodology. The results are presented in Sec. III. First, we describe the properties of equilibrium states. Next, we describe the self-assembly processes into bilayer vesicles. Discussion and conclusion are given in Secs. IV and V, respectively.

II. METHOD

An amphiphilic molecule is modeled as one hydrophilic particle ($j=1$) and two hydrophobic particles ($j=2,3$), which are separated by fixed distance σ and fixed on a line. Since solvent molecules are not taken into account explicitly, the hydrophobic interaction is mimicked by the multibody potential.

The motion of the jth particle of the ith molecule follows the underdamped Langevin equation,

$$m\frac{d^2\mathbf{r}_{i,j}}{dt^2}=-\zeta\frac{d\mathbf{r}_{i,j}}{dt}+\mathbf{g}_{i,j}(t)-\frac{\partial U}{\partial \mathbf{r}_{i,j}}, \tag{1}$$

where m is the mass of a particle and ζ is the friction constant. $\mathbf{g}_{i,j}(t)$ is Gaussian white noise and obeys the fluctuation-dissipation theorem,

$$\langle \mathbf{g}_{i,j}(t)\rangle=0, \quad \langle \mathbf{g}_{i,j}(t)\mathbf{g}_{i',j'}(t')\rangle=6k_{\mathrm{B}}T\zeta\delta_{ii'}\delta_{jj'}\delta(t-t'), \tag{2}$$

where k_{B} is the Boltzmann constant and T is the temperature. The equations of the translational and the rotational motion of molecules are integrated by leapfrog algorithm with a time step of $\Delta t=0.005$ or 0.01 [19].

Amphiphilic molecules ($i=1,\ldots,N$) interact by the repulsive soft core potential and the attractive ''hydrophobic'' potential,

$$U=\sum_{i\neq i'}U_{\mathrm{rep}}(|\mathbf{r}_{i,j}-\mathbf{r}_{i',j'}|)+\sum_{j=2,3}U_{\mathrm{hp}}(\rho_{i,j}). \tag{3}$$

Both particles have the same soft radius,

$$U_{\mathrm{rep}}(r)/\varepsilon=\exp\{-20(r/\sigma-1)\}, \tag{4}$$

where the cutoff length is 1.3σ. The multibody ''hydrophobic'' interaction is mimicked by the function $U_{\mathrm{hp}}(\rho)$ of the local density of hydrophobic particles.

 ©2001 The American Physical Society

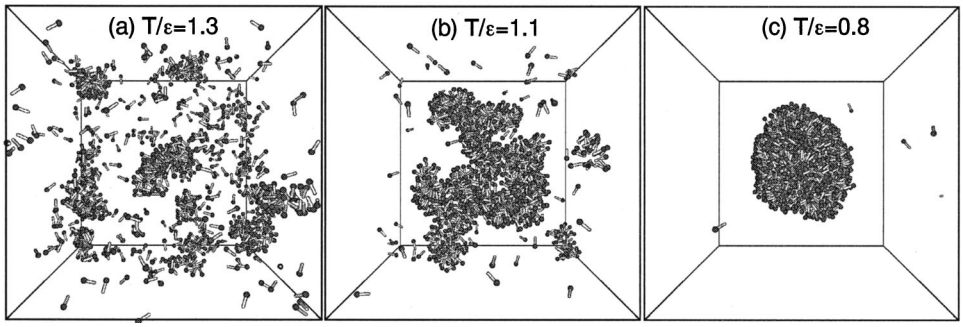

FIG. 1. Typical snapshots of 1000 amphiphilic molecules at various temperatures T: (a) Many small micelles at $T/\varepsilon=1.3$, (b) one or two large threadlike micelles at $T/\varepsilon=1.1$, and (c) one vesicle with bilayer structure at $T/\varepsilon=0.8$.

$$\rho_{i,j}=\sum_{i\neq i',j'=2,3} h(|\mathbf{r}_{i,j}-\mathbf{r}_{i',j'}|), \tag{5}$$

where

$$h(r)=\frac{1}{\exp\{20(r/\sigma-1.9)\}+1}.$$

$\rho_{i,j}$ is the number of hydrophobic particles in the sphere whose radius is approximately 1.9σ. We cut off the function $h(r)$ at 1.6σ and 2.2σ: $h(r)=1$ at $r<1.6\sigma$ and $h(r)=0$ at $r\geqslant 2.2\sigma$.

$U_{\rm hp}(\rho)$ is given by

$$U_{\rm hp}(\rho)/\varepsilon=\begin{cases}-0.5\rho & (\rho<\rho^*-1)\\ 0.25(\rho-\rho^*)^2-c & (\rho^*-1\leqslant\rho<\rho^*)\\ -c & (\rho^*\leqslant\rho).\end{cases} \tag{6}$$

We used the values $\rho^*=10$ and $c=4.75$ at $j=2$, $\rho^*=14$ and $c=6.75$ at $j=3$. At low density ($\rho<\rho^*-1$), $U_{\rm hp}(\rho)$ works as the pair-wise potential $-h(r)$. We assume that the particle is shielded by hydrophobic particles from solvent molecules and hydrophilic particles at ρ^*. Thus, $U_{\rm hp}(\rho)$ is constant at higher density ($\rho\geqslant\rho^*$).

We present our results with the reduced units, $\sigma=1$, $m=1$, $\zeta=1$, $\varepsilon=1$, $t_0=\zeta\sigma^2/\varepsilon=1$, and $k_{\rm B}=1$. We used the periodic boundary condition with the cubic box. We used low amphiphile concentration ($0.008/\sigma^3$) since our main target is vesicle: $N=1000$ and the side length of periodic boundary is 50σ. We checked that we obtained the equilibrium states using the two different types of initial states: For high temperature $0.9\leqslant T/\varepsilon\leqslant 1.2$, we have performed the annealing and slow heating simulations. For low temperature $T/\varepsilon\leqslant 0.8$, we have performed the annealing simulations and the simulations starting with flat bilayer membranes. We take the standard deviation of three to six separated runs as an estimate of the calculation error.

III. RESULTS

A. Equilibrium properties

The amphiphilic molecules aggregate to various morphologies dependent on the temperatures T. Figure 1 shows the snapshots at equilibrium states. As temperature decreases, the morphology of clusters changes from micelle to vesicle. We define a cluster as follows. When one of hydrophobic particles of a molecule is closer than 2σ with at least one of the hydrophobic particles of the molecules in a cluster, the molecule belongs to the cluster.

Figure 2 shows the distribution of cluster size $i_{\rm c}$ and the mean cluster size $m_{\rm c}$:

$$m_{\rm c}=\frac{\sum_{i_{\rm c}=1}^{\infty} i_{\rm c}n_{\rm c}}{\sum_{i_{\rm c}=1}^{\infty} n_{\rm c}}. \tag{7}$$

$n_{\rm c}$ is the number of molecules in the clusters of $i_{\rm c}$.

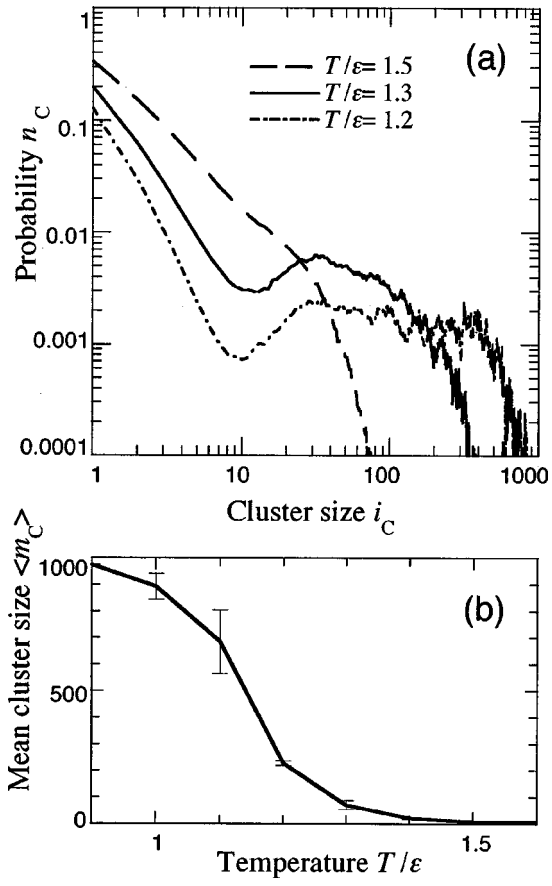

FIG. 2. Temperature dependence of the cluster size $i_{\rm c}$. (a) Probability distribution of the cluster size $i_{\rm c}$. (b) The mean cluster size $m_{\rm c}$ vs temperature T.

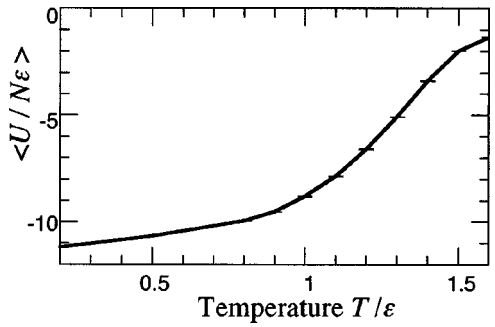

FIG. 3. Temperature dependence of the total energy U.

At $T/\varepsilon \geqslant 1.5$, n_c decreases with an increase in i_c. Most molecules exist alone and there is no characteristic cluster size. Thus, molecules are in random gas phase.

At $T/\varepsilon = 1.3$, n_c has a peak at $i_c = 30$. Some molecules aggregate to ellipsoidal or cylindrical micelles, and the others remain as random gas state [Fig. 1(a)]. These micelles frequently fuse and divide. As temperature decreases, the cluster size increases. At $T/\varepsilon = 1.1$, most molecules assemble into one or two large micelles. The micelles have branched threadlike shape [Fig. 1(b)]. This shape resembles that of the micelles of dimeric surfactants in the molecular dynamics study [20]. At $T/\varepsilon = 1$, the membranes form vesicles. However, these vesicles often have the defects such as pores and horns. They seem to be in sponge phase [1,2]. At $T/\varepsilon \leqslant 0.9$, the vesicles are stabilized. At $T/\varepsilon = 0.8$, one vesicle and a few isolated molecules exist [Fig. 1(c)]. At $T/\varepsilon \leqslant 0.5$, all molecules belong to one cluster. When an initial state is a flat bilayer membrane, the membrane forms vesicle at $0.05 \leqslant T/\varepsilon \leqslant 0.9$. At $T/\varepsilon = 0.025$, the membrane remains with flat disked shape at 50 000 time steps. It is likely caused by longer relaxation time.

Figure 3 shows the temperature dependence of the total energy U. As the mean cluster size m_c increases, U decreases at $0.9 \leqslant T/\varepsilon \leqslant 1.6$. At $T/\varepsilon \leqslant 0.9$, U decreases slower since vesicles exhibit more ordered bilayer structure. Figure 4 shows the sliced snapshot of a vesicle at $T/\varepsilon = 0.2$. Figure

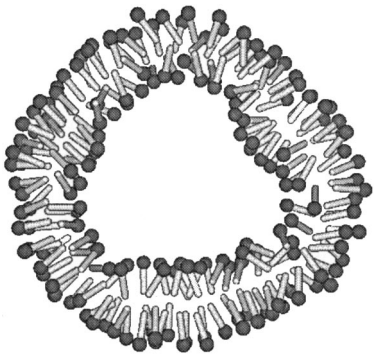

FIG. 4. Sliced snapshot of the vesicle consisting of 1000 molecules at temperature $T/\varepsilon = 0.2$. Molecules with $-1.5 < (\mathbf{r}_i - \mathbf{R}_g)\mathbf{e}_1 \leqslant 1.5$ are shown. $\mathbf{r}_i$ and $\mathbf{R}_g$ are the center of mass of ith molecule and the vesicle, respectively. $\mathbf{e}_1$, $\mathbf{e}_2$, and $\mathbf{e}_3$ (L_1^2, L_2^2, and L_3^2) are the eigenvectors (eigenvalues) of the moment tensor of inertia ($L_1 \leqslant L_2 \leqslant L_3$).

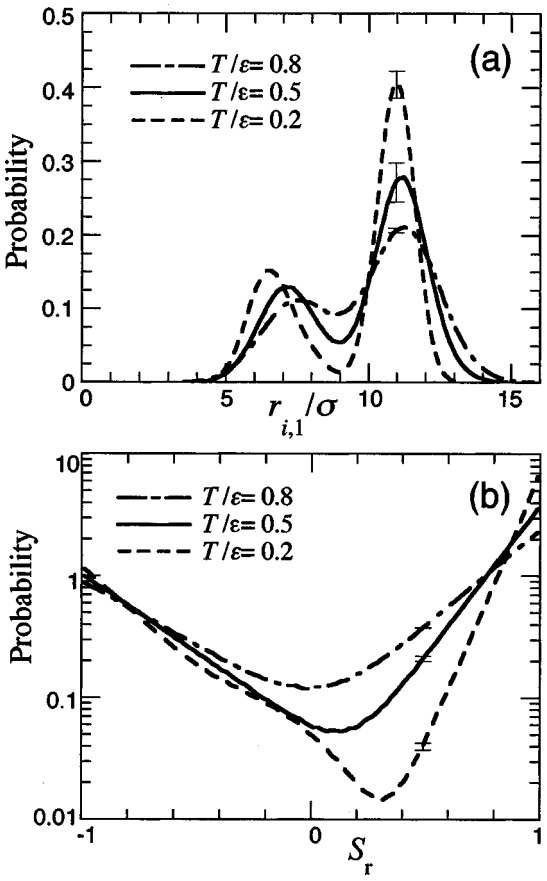

FIG. 5. (a) Probability distribution of the distance $r_{i,1}$ of hydrophilic particles from the center of mass of a vesicle. Error bars are shown only at $r_{i,1} = 10.95$. (b) The probability distribution of the degree of radial orientation S_r. Error bars are shown only at $S_r = 0.49$.

5(a) shows the radial distribution of hydrophilic particle positions $r_{i,1}$: $r_{i,1} = |\mathbf{r}_{i,1} - \mathbf{R}_G|$ where $\mathbf{R}_G$ is the center of mass of a vesicle. Two peaks represent inner and outer monolayers. The hydrophobic particles exist between two peaks. The number of molecules in inner monolayer is less than that in outer monolayer because inner monolayer has smaller radius. The double peak becomes sharper at lower temperature. Thus, the vesicles have clearer spherical symmetry and less deformed structures (see Fig. 4). At $T/\varepsilon = 0.8$ and 0.9, bilayer structures are deformed partially and a small pore occasionally opens on vesicles.

Figure 5(b) shows the degree of radial orientation S_r defined as $S_r = \mathbf{u}_i \mathbf{s}_i$. $\mathbf{u}_i$ is the unit orientation vectors of the ith molecule: $\mathbf{u}_i = (\mathbf{r}_{i,1} - \mathbf{r}_{i,3})/|\mathbf{r}_{i,1} - \mathbf{r}_{i,3}|$, where $\mathbf{r}_{i,1}$ and $\mathbf{r}_{i,3}$ are both ends of the molecule. $\mathbf{s}_i$ is the unit orientation vector of molecular position against $\mathbf{R}_G$: $\mathbf{s}_i = (\mathbf{r}_i - \mathbf{R}_G)/|\mathbf{r}_i - \mathbf{R}_G|$, where $\mathbf{r}_i$ is the center of mass of the ith molecule. The molecule, whose head is oriented to inside (outside), has negative (positive) S_r value. Thus, the probabilities of the molecules in inner and outer monolayers exhibit the peaks around $S_r = -1$ and 1 in Fig. 5(b), respectively.

We used these two quantities $r_{i,1}$ and S_r to distinguish inner and outer monolayers. When we calculate $r_{i,1}$, the molecules with $r_{i,1} \leqslant 9\sigma$ ($r_{i,1} > 9\sigma$) belong to inner (outer)

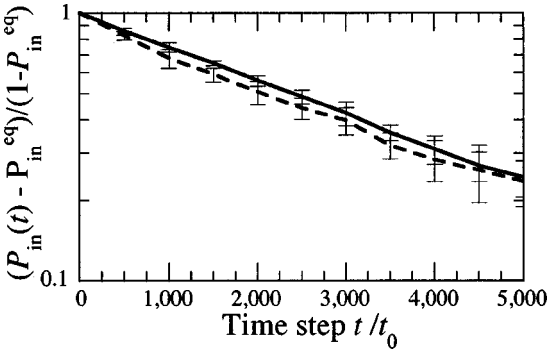

FIG. 6. Time development of the probability $P_{\rm in}(t)$ of molecules belonging to inner monolayer. $P_{\rm in}(t)$ is calculated for the molecules within inner monolayer at $t=0$. We estimate molecules within inner monolayer using $r_{i,1}$ (broken line) and $S_{\rm r}$ (solid line).

monolayer for vesicles with $i_{\rm c}\simeq 1000$. The threshold value is dependent on vesicle size. When we calculate $S_{\rm r}$, the threshold values are $S_{\rm r}=0.3$, 0.1, and -0.1 at $T/\varepsilon=0.2$, 0.5, and 0.8. They are weakly dependent on vesicle size. Here we define $P_{\rm in}^{\rm eq}$ as the probability of molecules within inner monolayer at equilibrium states. When we change $T/\varepsilon=0.2$, 0.5, and 0.8, we obtain the same values $P_{\rm in}^{\rm eq}=0.33(\pm 0.01)$ for $N=1000$ using both $r_{i,1}$ and $S_{\rm r}$. The classification using $r_{i,1}$ is clearer for smaller vesicles. We performed simulation of $N=2000$, and obtained ellipsoidal shaped vesicles. In this case, the above method using $r_{i,1}$ cannot be used.

We show the dynamical properties of vesicles. First, we evaluate the rate of flip-flop motion, which is the traverse motion between inner and outer monolayers. The differential equation of the probability $P_{\rm in}$ of molecules, which belong to the inner monolayer, is written as

$$\frac{dP_{\rm in}}{dt}=-k_{\rm out}P_{\rm in}+k_{\rm in}P_{\rm out}, \tag{8}$$

where $P_{\rm in}+P_{\rm out}=1$ [21]. $k_{\rm out}$ is the rate constant of flop motion, traverse from the inner to outer monolayer, and $k_{\rm out}$ is that of flip motion, opposite traverse. The equilibrium probability is derived as $P_{\rm in}^{\rm eq}=k_{\rm in}/(k_{\rm in}+k_{\rm out})$. At $0.2\leqslant T/\varepsilon\leqslant 0.8$ and $N=1000$, $k_{\rm out}$ equals $2k_{\rm in}$ because of $P_{\rm in}^{\rm eq}=0.33$. Eq. (8) is integrated to

$$\frac{P_{\rm in}(t)-P_{\rm in}^{\rm eq}}{P_{\rm in}(0)-P_{\rm in}^{\rm eq}}=\exp[-(k_{\rm in}+k_{\rm out})t]. \tag{9}$$

Figure 6 shows the relaxation $P_{\rm in}(t)$ of molecules within inner monolayer at $t=0$. The exponential decrease in $P_{\rm in}(t)$ agrees with Eq. (9). $P_{\rm in}(t)$ evaluated from $r_{i,1}$ and $S_{\rm r}$ coincides within the statistical error. Thus, the half-lifetime of flip and flop motion at $T/\varepsilon=0.5$ is evaluated as 8000 (± 2000) and 4000 (± 1000) time steps from Fig. 6, respectively. The rate of flip-flop motion decreases largely with a decrease in temperature. At $T/\varepsilon=0.2$, flip-flop motion is much slower: The half-lifetime of flop motion is 200 000 ($\pm 100\,000$) and 400 (± 50) time steps at $T/\varepsilon=0.2$ and 0.8, respectively.

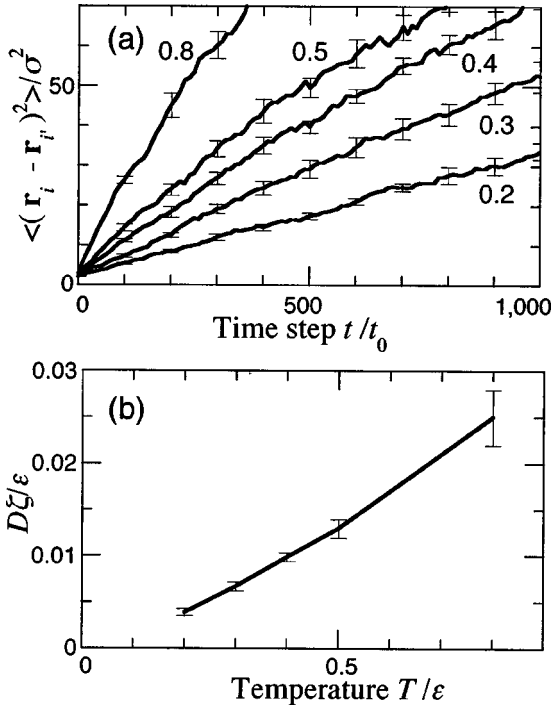

FIG. 7. Lateral diffusion. (a) Time development of the distance of two molecules, which started as neighboring molecules at $t=0$. The numbers in the figure are temperatures T/ε. Error bars are shown for ten data points. (b) Temperature dependence of the lateral diffusion constant D.

Next, we evaluate the lateral diffusion constant D. Figure 7(a) shows the time development of the mean squared separation of two initially neighboring molecules $\langle(\mathbf{r}_i-\mathbf{r}_{i'})^2\rangle$. They are proportional to time steps. Since flip-flop motion is slower, these separations are mainly due to the lateral diffusion. Figure 7(b) shows the lateral diffusion constant D. We evaluate it from $\langle(\mathbf{r}_i-\mathbf{r}_{i'})^2\rangle=8Dt$, since two molecules diffuse on the two-dimensional surface, D is roughly proportional to T. Thus, the vesicles are in fluid phase at $0.2\leqslant T/\varepsilon\leqslant 0.8$, and the molecules diffuse in the lateral and traverse directions.

B. Self-assembly kinetics

In this section, we describe the self-assembly processes from random gas states at $T/\varepsilon=1.5$ into bilayer vesicles. Figures 8 and 9 show an example of the self-assembly process at $T/\varepsilon=0.5$. First, the amphiphilic molecules aggregate to small clusters. They have spherical or ellipsoidal shape. They then assemble into larger clusters. Finally, two vesicles are obtained at $t=50\,000$. At $T/\varepsilon=0.5$, sphere is the stable morphology of clusters of $i_{\rm c}>10$. The stable structures of clusters change from spherical micelles to spherical vesicles through the middle structure, semivesicle. The clusters of middle size ($40<i_{\rm c}<200$) consist of the outer monolayer and the inner inverted micelle [see the left cluster in Fig. 8(d′)]. As $i_{\rm c}$ increases, the number of molecules in the in-

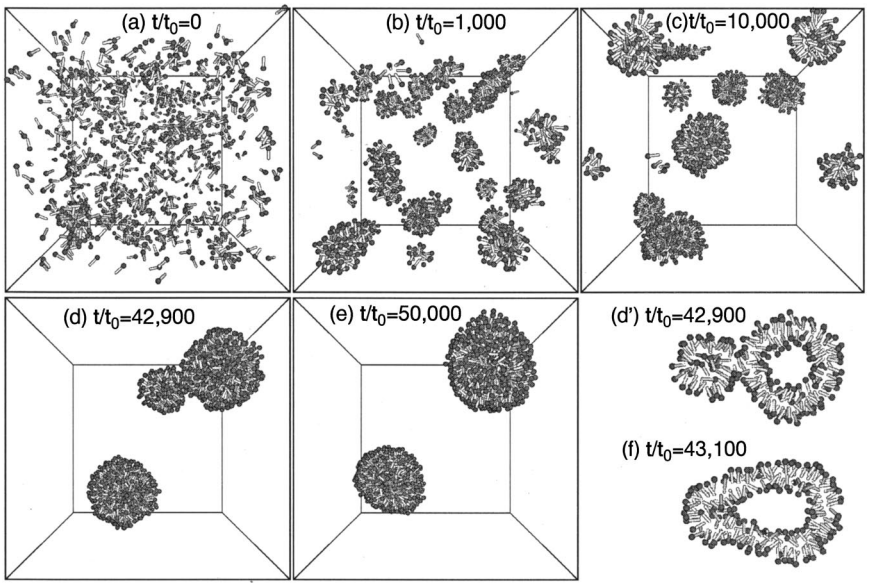

FIG. 8. Snapshots of the self-assembly process at temperature $T/\varepsilon=0.5$. The initial state is the random gas states at $T/\varepsilon=1.5$. (d′,f) The sliced snapshots of the right cluster shown in (d). The depiction of snapshots of (d′) and (f) is the same as that of Fig. 4.

verted micelle increases. Thus, the stable structure changes continuously from micelle to vesicle. Figures 8(d), 8(d′), and 8(f) show the fusion process of two clusters with $i_c=114$ and 416. First, the outer monolayers of the contacted clusters are connected [Figs. 8(d) and 8(d′)]. This structure is similar to the stalk intermediate [5,6,22], and has short lifetime of 600 time steps. Immediately, the connection part expands radially and the inner monolayer and inverted micelle are connected [Fig. 8(f)]. The radius of gyration R_g of the contacted vesicles [Figs. 8(d) and 8(d′)] is larger than R_g of the spherical vesicle with same cluster size. The fast decreases of R_g after fusions as shown in Fig. 9(b) indicate the fast relaxation into spherical vesicles.

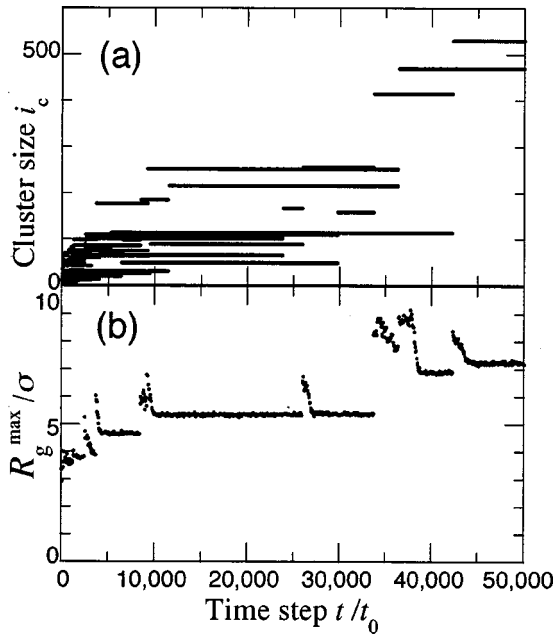

FIG. 9. Time development of (a) the cluster size i_c and (b) the radius of gyration of the cluster of maximum size R_g^{max} at $T/\varepsilon=0.5$ for the same data shown in Fig. 8.

Figure 10 shows the time development of the mean cluster size $\langle m_c\rangle$ averaged for ten separated runs. Clusters grow faster at higher temperature. At all temperatures, m_c increases as t^{α}, where $\alpha=0.5\pm0.1$.

The fusion processes and the relaxation into stable structures of clusters are slower at $T/\varepsilon=0.2$ than those at $T/\varepsilon=0.5$. The disk-shaped micelles have a finite lifetime.

At $T/\varepsilon=0.8$, the clusters have more disordered structures by the thermal fluctuation. The fusion of vesicles is often accompanied by the deformation of vesicles. These vesicles exhibit occasionally bowl-shaped conformation. At $i_c\simeq100$, disk-shaped micelle or bilayer membrane with edge is more stable than spherical semivesicle. When the cluster size becomes a few hundred, the cluster forms vesicle. Figure 11 shows the vesicle formation of the cluster of $i_c\simeq300$. The membrane bends into a vesicle through undulated bowl-shaped conformation. A similar relaxation process is observed at $T/\varepsilon=0.2$ and 0.5, when the initial state is a flat

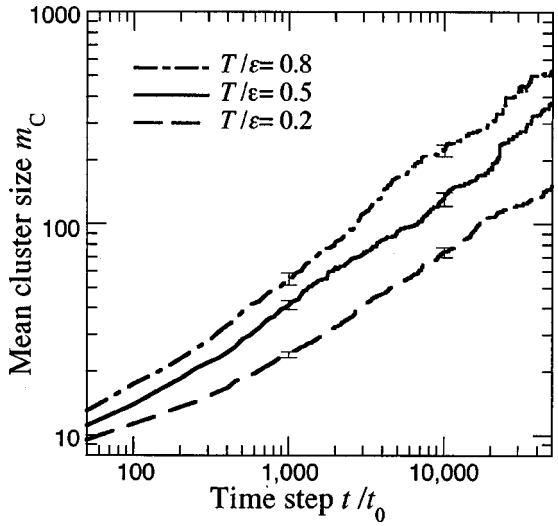

FIG. 10. Time development of the mean cluster size $\langle m_c\rangle$ at $T/\varepsilon=0.2$, 0.5, and 0.8. Error bars are shown for 200 data points.

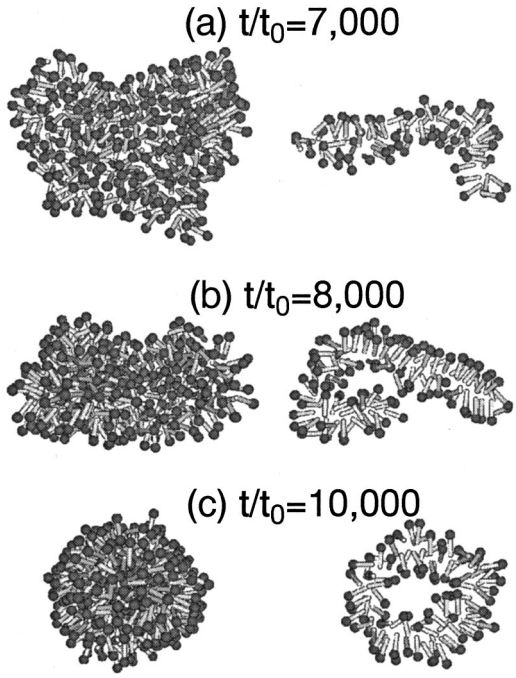

FIG. 11. Snapshots of the vesicle formation with $i_c \simeq 300$ at temperature $T/\varepsilon = 0.8$. The left parts show all molecules within the cluster viewed from $\mathbf{e}_1$ direction. The right parts show the sliced snapshots viewed from $\mathbf{e}_2$ direction, where molecules with $-1.5 < (\mathbf{r}_i - \mathbf{R}_g)\mathbf{e}_2 \leqslant 1.5$ are shown.

bilayer membrane with $i_c = 1000$. However, they have more axial symmetrical structures.

IV. DISCUSSION

We used the multibody potential $U_{hp}(\rho)$ for ''hydrophobic'' interaction. If the pair-wise potential $-\varepsilon h(r)$ is used instead of $U_{hp}(\rho)$ (or $\rho^* = \infty$), the bilayer membrane has no fluid phase and forms no vesicle spontaneously. Thus, the property of multibody is significant for the simulation of vesicle formation. In our present model, vesicles are in fluid phase in wide temperature region $0.2 \leqslant T/\varepsilon \leqslant 0.8$. It is well known that the phospholipid membranes exhibit the transition from fluid phase to gel phase, where the molecules diffuse little, with a decrease in temperature [23,24]. On the other hand, the membranes consisting of phospholipid and cholesterol do not exhibit discrete fluid-gel transition. Our present model may be rather close to the latter membranes. The fluid-gel transition might be observed using the adequate larger values of ρ^*.

We used rigid amphiphilic molecules with fixed length. The properties of vesicles would depend on the length and stiffness of molecules. When longer molecules are used, the neighboring molecules may be more oriented, and the flip-flop motion may be slower. Recently, the vesicles consisting of fullerene-based surfactants were observed by light scattering [25]. This molecule has rigid hydrophobic ball. On the other hand, phospholipid molecules have flexible hydrophobic chains. Both stiff and flexible amphiphilic molecules form vesicles in experiments. Our model does not take into account explicit solvent molecules, and the osmotic pressure of the simulated vesicles is always zero. Under the osmotic pressure, the vesicles exhibit various morphologies such as discocyte and dumbbell [1,2,7]. The estimation of inside volume of vesicles is needed to take into account the osmotic pressure in our model. The further developments of simulation model are needed to clarify these effects.

To examine the fusion process is important biologically. In Ref. [22], we have clarified the fusion pathways of two vesicles with $i_c = 500$ at $T/\varepsilon = 0.2$ and 0.5. First, the contacted vesicles form a stalk intermediate, a necklike structure connecting only outer monolayers. The stalk intermediates have longer lifetime than 10 000 time steps. At $T/\varepsilon = 0.2$, the stalk expands radially and the inner monolayers contact inside of the stalk. This contact leads to fusion-pore opening. These processes support the modified stalk model [6]. On the other hand, at $T/\varepsilon = 0.5$, the fusion pore opens through a different pathway. The stalk bends, and the cross-section shape of the stalk changes from ellipse to arc. The pore connecting the inside and outside of a vesicle opens by side of the stalk. The contacted ends of arc-shaped stalk form the fusion pore connecting the insides of vesicles. In our present paper, we show the fusion of semivesicle in self-assembly processes at $T/\varepsilon = 0.2$ and 0.5. They fuse mainly through the pathway in the modified stalk model. These stalk intermediates have a lifetime shorter than 3000 time steps, since semivesicles are less stable than vesicles. The fusion pathway of vesicles at $T/\varepsilon = 0.8$ is similar to stalk-bending process at $T/\varepsilon = 0.5$. However, it involves more disordered structures. At $T/\varepsilon = 0.8$, pores on a vesicle occasionally open even in equilibrium state, while at $T/\varepsilon = 0.5$ the pores open only by the side of the stalk. In vesicle fusion at $T/\varepsilon = 0.8$, large pores on vesicles often open, the reconnection of bilayer membranes occurs.

In the self-assembly of amphiphilic molecules, the cluster size increases as $m_c \propto t^{0.5}$. The characteristic length of the clusters shows $t^{0.2}$ development since the clusters are in three-dimensional space. Many theoretical and experimental studies show that the characteristic length exhibits t^{α} development in spinodal decomposition [26,27]. $t^{0.2}$ development is reported for solid systems [26]. In our simulation, we use Brownian dynamics and ignore hydrodynamic interaction. Thus, the diffusion constant of clusters obeys $\propto i_c^{-1}$. Our results should agree with spinodal decomposition in solid systems rather than fluid systems. When the model includes hydrodynamic interaction, the characteristic length likely exhibits $t^{1/3}$ development of ordinary spinodal decomposition in fluid systems.

V. CONCLUSION

We have proposed a simple model of amphiphilic molecules to investigate vesicles with bilayer structure. We have studied the equilibrium properties and self-assembly processes of amphiphilic molecules. As temperature decreases, the amphiphilic molecules aggregate to larger clusters and the morphologies of clusters change from spherical and threadlike micelles to vesicles. The vesicles are in fluid phase, and the diffusions of lateral and traverse directions are observed.

At $T/\varepsilon = 0.2$, 0.5, and 0.8, the amphiphilic molecules self-assemble into vesicles from random gas states. First, the small micelles are formed and then they assemble and reform to vesicles. The mean cluster size m_c increases as $t^{0.5}$.

ACKNOWLEDGMENT

This work was supported in part by a Grant-in-Aid for Scientific Research from the Ministry of Education, Culture, Sports, Science, and Technology of Japan.

[1] *Structure and Dynamics of Membranes*, edited by R. Lipowsky and E. Sackmann (Elsevier Science, Amsterdam, 1995).
[2] R. Lipowsky, Nature (London) **349**, 475 (1991).
[3] R. Jahn and T.C. Südhof, Annu. Rev. Biochem. **68**, 863 (1999).
[4] L.D. Hernandez, L.R. Hoffman, T.G. Wolfsberg, and J.M. White, Annu. Rev. Cell Dev. Biol. **12**, 627 (1996).
[5] L. Chernomordik, M.M. Kozlov, and J. Zimmerberg, J. Membr. Biol. **146**, 1 (1995).
[6] D.P. Siegel, Biophys. J. **65**, 2124 (1993).
[7] H. Hotani, F. Nomura, and Y. Suzuki, Curr. Opin. Colloid Interface Sci. **4**, 358 (1999).
[8] T. Umeda, H. Nakajima, and H. Hotani, J. Phys. Soc. Jpn. **67**, 682 (1998).
[9] Y. Suezaki, H. Ichinose, K. Takiguchi, and H. Hotani, Biophys. Chem. **80**, 119 (1999).
[10] R.W. Pastor, Curr. Opin. Struct. Biol. **4**, 486 (1994).
[11] D.P. Tieleman, S.J. Marrink, and H.J.C. Berendsen, Biochim. Biophys. Acta **1331**, 235 (1997).
[12] W. Shinoda, N. Namiki, and S. Okazaki, J. Chem. Phys. **106**, 5731 (1997).
[13] Y. Takaoka *et al.*, Biophys. J. **79**, 3118 (2000).
[14] R. Goetz, G. Gompper, and R. Lipowsky, Phys. Rev. Lett. **82**, 221 (1999).
[15] J.-M. Drouffe, A.C. Maggs, and S. Leibler, Science **254**, 1353 (1991).
[16] R. Morikawa and Y. Saito, J. Phys. II **4**, 145 (1994).
[17] D. Brindle and C.M. Care, J. Chem. Soc., Faraday Trans. **88**, 2163 (1992).
[18] A.T. Bernardes, J. Phys. II **6**, 169 (1996); Langmuir **12**, 5763 (1996).
[19] M.P. Allen and D.J. Tildesley, *Computer Simulation of Liquids* (Clarendon Press, Oxford, 1987).
[20] S. Karaborni *et al.*, Science **266**, 254 (1994).
[21] R.D. Kornberg and H.M. McConnell, Biochemistry **10**, 1111 (1971).
[22] H. Noguchi and M. Takasu (unpublished).
[23] E.-S. Wu, K. Jacobson, and D. Papahadjopoulos, Biochemistry **16**, 3936 (1977).
[24] M.R. Vist and J.H. Davis, Biochemistry **29**, 451 (1990).
[25] S. Zhou *et al.*, Science **291**, 1944 (2001).
[26] H. Furukawa, Adv. Phys. **34**, 703 (1985).
[27] Y. Oono and S. Puri, Phys. Rev. A **38**, 434 (1988).